Journal of Nuclear Materials 406 (2010) 257–262

Contents lists available at ScienceDirect

Journal of Nuclear Materials

journal homepage: www.elsevier.com/locate/jnucmat

Study of PRIMAVERA steel samples by a positron annihilation spectroscopy technique

V. Grafutin [a], O. Ilyukhina [a], V. Krsjak [b,*], R. Burcl [b], P. Hähner [b], D. Erak [c], A. Zeman [b]

[a] Institute of Theoretical and Experimental Physics, B. Cheremushkinskaya 25, 117218 Moscow, Russia
[b] European Commission, Joint Research Centre, Institute for Energy, P.O. Box 2, 1755 ZG Petten, The Netherlands
[c] RRC Kurchatov Institute, Kurchatov Square 1, 123182 Moscow, Russia

ARTICLE INFO

Article history:
Received 4 February 2010
Accepted 28 August 2010

ABSTRACT

In the present article, a positron annihilation spectroscopy investigation of VVER-440/230 weld materials is discussed. Important characteristics of metals such as Fermi energy, concentration of electrons in the conduction band, size and concentration of defects were experimentally determined for three model materials with higher level of copper (0.16 wt.%) and phosphorus (0.027–0.038 wt.%). The impact of neutron irradiation and subsequent annealing on crystal lattice parameters was investigated. The experiments with the angular correlation of positron annihilation radiation (ACAR) complement the published positron annihilation spectroscopy (PAS) studies of the radiation treated VVER materials as well as previous experiments on PRIMAVERA materials. The availability of the experimental reactor to prepare strong ^{64}Cu positron sources provided for unique experimental conditions, such as good resolution of spectra (0.4 mrad) and reasonable short time of measurement (36 h). The present paper aims to contribute to further understanding of RPV (reactor pressure vessel) steels behaviour under irradiation conditions as well as annealing recovery procedures, which have already been applied at several VVER NPP units in Europe.

1. Introduction

Extending of the operational lifetime of the current generation of nuclear reactors is a reasonable way to respond to future energy demands and CO_2 reduction requirements, which may occur as a result of the expected shut down of Generation II nuclear power plants (NPP) and delayed commissioning of new nuclear units (Generation II+ and III). It is well known that one of the most critical components for life extension is the reactor pressure vessel (RPV). Degradation of mechanical properties during operation, caused predominantly by radiation embrittlement of the RPV steel, is more significant in Russian-designed types of PWR (VVER-440, in particular, type 230), where the gap between the surface of the reactor core internals and the inside surface of the RPV is narrower than in Western PWRs [1].

Given the large number of NPPs of VVER type, annealing procedures have been developed and practically applied to eliminate the consequences of RPV material embrittlement and to recover the original properties of structural materials, to permit extension of NPP lifetimes.

However, in order to predict RPV steel properties, establish annealing procedures and properly justify lifetime extension, it is necessary to have a detailed understanding of the embrittlement and annealing processes and to develop a model describing the properties and behaviour of the materials in question. The international project PRIMAVERA studies the mechanical properties of the materials and the properties and behaviour of nanoscale objects (defects) under irradiation and post-irradiation annealing conditions. The most typical RPV materials used at VVER plants have been chosen for this investigation [2].

Reports on the mechanical properties and atom probe tomography studies of irradiated, annealed and re-irradiated materials in comparison to the original properties already exist [2,3]. Nevertheless, more detailed information is needed on nanoscale objects and effects in order to develop the model describing the processes studied. For this reason radiation damage studies should include additional complementary tests [4]. One of the techniques suitable for this purpose is the positron annihilation spectroscopy (PAS).

Positron annihilation spectroscopy is a powerful tool to study nano-objects (defects) in radiation treated materials [5–7]. Combination of various PAS techniques — angular correlation positron annihilation spectroscopy (ACAR), positron lifetime measurement (LT) and measurement of Doppler broadening of the annihilation line (DB) — allows to obtain more detailed and complex qualitative and quantitative characterization of nano-objects. There is also a large number of published experiments on the applied surface

* Corresponding author. Tel.: +31 224 565395.
E-mail address: vladimir.krsjak@ec.europa.eu (V. Krsjak).

0022-3115/$ - see front matter © 2010 Elsevier B.V. All rights reserved.
doi:10.1016/j.jnucmat.2010.08.046

science, where the slow positron beam technique (e.g. PLEPS) has been used [6,8–10].

PAS-ACAR results for the PRIMAVERA samples are discussed in this paper, together with the published results of other PAS techniques (LT and DB) for the same type of materials. Positron lifetime study of the PRIMAVERA samples is foreseen for 2010 and a comprehensive analysis of all experimental results will be presented in follow-up articles.

2. Experiment

Three different VVER-440 weld materials were investigated in the (i) unirradiated, (ii) irradiated (two different neutron fluence levels), and (iii) irradiated and annealed state. These materials differ in phosphorus content (which is considered to be one of critical parameters for radiation embrittlement) and their chemical composition can be seen in Table 1. All available information about manufacturing and pre-irradiation treatment of the materials can be found in [2]. It is important to note both, the higher phosphorus and copper content, as compared to conventional VVER-440 weld (Sv-10KhFMT, WM) and base (15Kh2MFA, BM) material. The role of copper precipitation and phosphorus segregation in the radiation embrittlement has been discussed earlier [e.g. 8,9]. Although impact of copper and phosphorus was not directly observed in the present study, one of the aims of our work was to use unique abilities of the ACAR technique in the characterization of the crystal lattice, which might be, after radiation treatment, affected by the chemical composition.

Irradiation of the PRIMAVERA materials has been performed by Russian Research Centre, Kurchatov Institute (RRC KI). Bulk samples ($10 \times 10 \times 18$ mm) were irradiated at 270 °C with a neutron flux of 2×10^{12} cm^{-2} s^{-1} in the surveillance channels of Rovno NPP (Ukraine) for one or 3 years respectively. The neutron fluencies for individual samples are depicted in Fig. 1. After 3 years of irradiation, one set of samples was annealed using the standard annealing procedure for VVER-440 RPV (475 °C/100 h). For PAS experiments the samples $10 \times 10 \times 1$ mm were prepared from original bulk samples.

Our study of model VVER-440 weld materials also took account of the published PAS experiments of Kocik et al. [11] and Slugen et al. [8]. As can be seen in Fig. 2, the present work is complementary to previous work, so our interpretation of the results is based on three different positron annihilation spectroscopy techniques including conventional 3-detector PAS-LT, PLEPS [12] and PAS-ACAR.

The angular correlation experiments were carried out at the Moscow Institute of Physical Engineering (MIPhE) using the typical set-up of one-dimensional ACAR [13]. ^{64}Cu was used as the source of positrons in this study. Individual positron sources were made from electrolytic copper foil, size $10 \times 10 \times 2$ mm. The foils were irradiated for 24 h in the IRT-2000 reactor (MIPhE) at neutron flux 2×10^{13} cm^{-2} s^{-1} and the positron sources with an activity of ~0.1TBq were immediately placed in the ACAR facility. In spite of high activity of positron sources, due to the short half-life of ^{64}Cu (12.7 h), each measurement cycle lasts only 36 h. Experimental spectra were measured with angular resolution of 0.4 mrad and $(10–15) \times 10^4$ of total count at the peak maximum.

Table 1
Chemical composition (in wt.%) of the investigated PRIMAVERA steel samples with low, medium and high (LP, MP, HP) phosphorus content, conventional VVER-440 base 15Kh2MFA (BM) and weld Sv-10KhFMT (WM) material (Fe balance).

	C	Si	Mn	P	S	Cr	Ni	Mo	Cu	V
LP	0.04	0.04	1.12	0.027	0.013	1.42	0.13	0.49	0.16	0.19
MP	0.04	0.39	1.15	0.031	0.013	1.42	0.13	0.50	0.16	0.18
HP	0.05	0.36	1.09	0.038	0.014	1.54	0.13	0.51	0.16	0.19
WM	0.04	0.59	1.1	0.012	0.017	1.37	–	0.50	0.06	0.20
BM	0.16	0.17	0.46	0.014	0.016	2.9	0.07	0.66	0.07	0.31

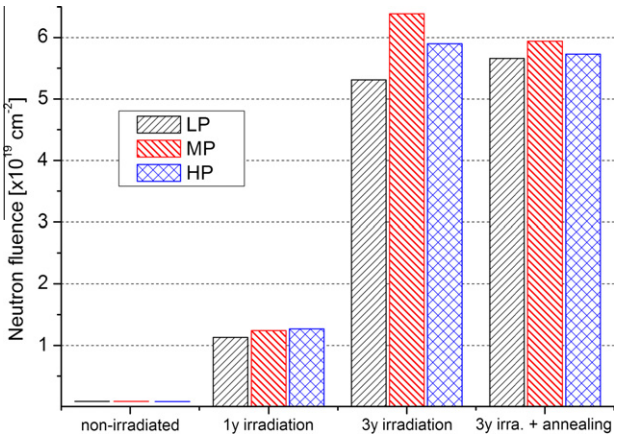

Fig. 1. Irradiation characteristics of the investigated PRIMAVERA steel samples.

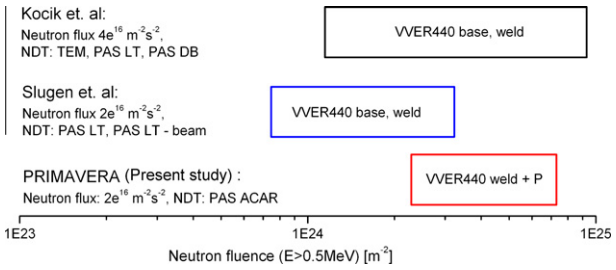

Fig. 2. PAS experiments published on VVER-440 materials, neutron fluence characteristics and non-destructive techniques used [8,11].

3. Results and discussion

In general, positrons annihilate in metals and alloys with electrons from the conduction band and the electrons from the localized ion electron shell. Annihilation with delocalized conduction electrons results in a parabolic component of ACAR spectra, while annihilation with localized electrons results in a Gaussian component [14]. Processing of the experimental results shows the density of electrons in the conduction band, the Fermi energy, the size and type of defects and also their topology.

For interpretation of the spectra we used both models with two components (one Gaussian, one parabolic) and models with three components (two Gaussians, one parabolic). The calculations were carried out using the program ACARFIT of the data-processing system PATFIT-88 [15]. As can be seen in Fig. 3 and Tables 2–4, the three-component model fit describes the experimental spectra very well and the uncertainty is lower ($\chi^2 \sim 0.6$) compared with the two-component model ($\chi^2 \sim 1.8$). The results of ACAR parameters based on the two and three-component model are compiled in the Tables 2–4 for LP, MP and HP respectively. Graphical representation of the data (three-component model) can be seen in Figs. 4a and 4b, 5a and 5b, 6a and 6b. Annealed states are here designated with an asterisk (*) and follow the actual dose level.

With a reasonable level of approximation, i.e. (i) defects are modelled as potential wells with infinitely high walls, (ii) positrons are considered to be thermalised, and (iii) spherical geometry of the open volume defects, we can assign the narrower Gaussian ($\Gamma_{g1} \sim 8.62 - 11.6$ mrad) component to the annihilation with valence electrons of atoms, the wider Gaussian ($\Gamma_{g2} \sim 14 - 18.8$

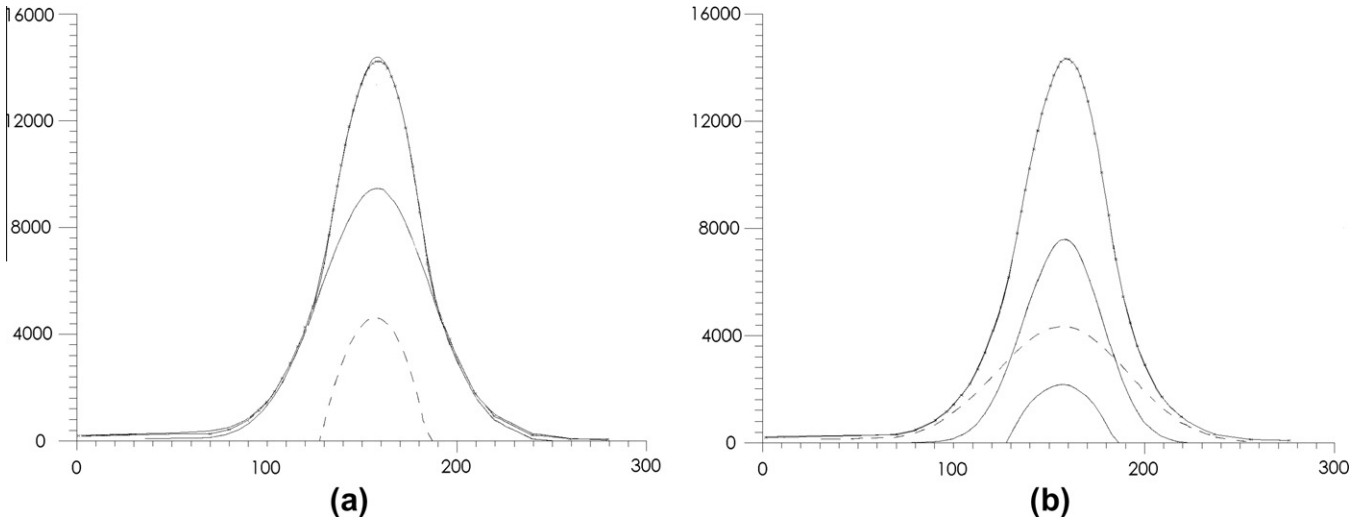

Fig. 3. Decomposition of experimental spectra into Gaussian and parabolic (a) and two Gaussians and parabolic (b) components.

Table 2
Results of ACAR spectra decompositions (2 and 3 component model), LP steel.

Treatment of the specimen	Γ_{g1} (mrad)	S_{g1}/S_{sum} (%)	E_{g1} (eV)	Γ_{g2} (mrad)	S_{g2}/S_{sum} (%)	E_{g2} (eV)	Γ_p (mrad)	S_p/S_{sum} (%)	E_F (eV)	N_p (θ) (1022 cm−3)
Non-irradiated	13.20	82.94	12.00	N/A for two-component model			5.74	17.06	8.41	11.2
	±0.07	±3.00	±0.01					±1.10	±0.88	
Non-irradiated	10.00	53.15	6.91	16.40	40.61	18.60	5.97	6.24	9.08	12.6
	±0.38	±14.00	±0.05	±0.60	±15.00	±0.08		±2.70	±5.10	
Irradiated (12.2×10^{18})	13.60	79.01±	12.80	N/A			5.65	20.99	8.13	10.6
	±0.07	±3.20	±0.01					±1.00	±0.43	
Irradiated (12.2×10^{18})	9.39	42.80	6.09	16.20	48.74	18.10	5.63	8.46	8.07	10.5
	±0.39	±11.00	±0.05	±0.47	±14.00	±0.07		±2.90	±3.30	
Irradiated (59.5×10^{18})	13.30	78.97±	12.20	N/A			5.60	21.03	8.00	10.4
	±0.07	±2.80	±0.01					±0.87	±0.37	
Irradiated (59.5×10^{18})	8.94	34.69	5.52	15.00	55.63	15.50	5.61	9.68	8.02	10.4
	±0.37	±9.10	±0.05	±0.33	±14.00	±0.05		±2.70	±2.40	
Irradiated (57.1×10^{18}) and annealed	13.20	79.73	12.10	N/A			5.37	20.27	7.36	9.2
	±0.06	±2.40	±0.01					±0.74	±0.31	
Irradiated (57.1×10^{18}) and annealed	11.60	63.65	9.23	18.80	20.80	24.40	5.31	15.54	7.18	8.8
	±0.40	±17.00	±0.06	±1.70	±14.00	±0.23		±3.60	±0.82	

Γ_{gi} – FWHM of the Gaussian component (i = 1 for narrower, i = 2 for wider component, respectively) Γ_p – angle of cutoff of the θ–axis (angle) by the parabola; E_{gi} – energy of the annihilating pair, i = 1, 2; $S_{gi}/S_p/S_{sum}$ – area under Gaussian/parabola/total area, i = 1, 2; E_F – Fermi energy; N_p (θ) – density of the conduction band electrons.

Table 3
Results of the ACAR spectra decompositions (2 and 3 component model), MP steel.

Treatment of the specimen	Γ_{g1} (mrad)	S_{g1}/S_{sum} (%)	E_{g1} (eV)	Γ_{g2} (mrad)	S_{g2}/S_{sum} (%)	E_{g2} (eV)	Γ_p (mrad)	S_p/S_{sum} (%)	E_F (eV)	N_p (θ) (10^{22}cm^{-3})
Non-irradiated	13.40	79.07	12.40	N/A			6.03	20.93	9.26	13
	±0.09	±3.60	±0.01					±1.20	±0.59	
Non-irradiated	9.97	48.06	6.86	16.10	42.53	17.90	6.09	9.40	9.45	13.3
	±0.42	±15.00	±0.06	±0.59	±16.00	±0.08		±3.40	±3.70	
Irradiated (12.4×10^{18})	13.90	77.70	13.30	N/A			5.66	22.30	8.17	10.7
	±0.08	±2.90	±0.01					±0.93	±0.37	
Irradiated (12.4×10^{18})	9.14	46.23	5.76	15.90	47.55	17.50	5.81	6.21	8.62	11.6
	±0.29	±11.00	±0.04	±0.45	±13.00	±0.06		±2.50	±4.70	
Irradiated (63.9×10^{18})	13.30	79.37	12.20	N/A			5.64	20.63	8.12	10.6
	±0.09	±3.50	±0.01					±1.10	±0.49	
Irradiated (63.9×10^{18})	9.16	35.85	5.79	15.90	53.77	17.40	5.68	10.39	8.23	10.8
	±0.40	±9.20	±0.06	±0.38	±13.00	±0.05		±3.00	±2.70	
Irradiated (59.4×10^{18}) and annealed	12.90	83.76	11.50	N/A			5.35	16.24	7.29	9.0
	±0.08	±3.30	±0.01					±0.92	±0.52	
Irradiated (59.4×10^{18}) and annealed	9.79	57.04	6.61	16.70	38.09	19.30	5.14	4.87	6.73	8.0
	±0.38	±14.00	±0.05	±0.67	±14.00	±0.09		±2.30	±4.40	

Γ_{gi} – FWHM of the Gaussian component, i = 1, 2; Γ_p – angle of cutoff of the θ–axis (angle) by the parabola; E_{gi} – energy of the annihilating pair, i = 1, 2; $S_{gi}/S_p/S_{sum}$ – area under Gaussian/parabola/total area, i = 1, 2; E_F – Fermi energy; N_p (θ) – density of the conduction band electrons.

mrad) to the annihilation with core electrons of the ions and the parabolic component Γ_p (the angle of cut-off of the Γ-axis by the parabola) to annihilation with conduction band (free) electrons [16,17].

Table 4
Results of the ACAR spectra decompositions (2 and 3 component model), HP steel.

Treatment of the specimen	Γ_{g1} (mrad)	S_{g1}/S_{sum} (%)	E_{g1} (eV)	Γ_{g2} (mrad)	S_{g2}/S_{sum} (%)	E_{g2} (eV)	Γ_p (mrad)	S_p/S_{sum} (%)	E_F (eV)	$N_p(\theta)$ (10^{22} cm^{-3})
Non-irradiated	13.20	81.69	12.30	N/A			6.00	18.31	9.18	12.8
	±0.09	±3.00	±0.01					±1.20	±0.71	
Non-irradiated	9.21	39.33	5.86	15.00	56.05	15.60	6.29	4.62	10.10	14.8
	±0.40	±14.00	±0.06	±0.44	±11.00	±0.06		±2.70	±8.00	
Irradiated (12.2×10^{18})	13.90	75.09	13.30	N/A			6.00	24.91	9.18	12.8
	±0.07	±2.40	±0.01					±0.83	±0.32	
Irradiated (12.2×10^{18})	10.00	42.42	6.92	16.50	43.69	18.70	5.98	13.90	9.13	12.7
	±0.33	±9.20	±0.05	±0.42	±11.00	±0.06		±2.90	±1.60	
Irradiated (59.5×10^{18})	13.40	79.34	12.50	N/A			5.71	20.66	8.31	11.0
	±0.07	±2.60	±0.01					±0.82	±0.38	
Irradiated (59.5×10^{18})	8.62	27.37	5.12	14.00	64.20	13.5	5.71	8.43	8.31	11.0
	±0.57	±12.00	±0.08	±0.35	±20.00	±0.05		±3.50	±4.00	
Irradiated (57.1×10^{18}) and annealed	13.80	77.60	13.10	N/A			5.65	22.40	8.13	10.7
	±0.09	±3.10	±0.01					±0.99	±0.39	
Irradiated (57.1×10^{18}) and annealed	9.24	43.22	5.89	16.20	49.24	18.00	5.55	7.54	7.85	10.1
	±0.35	±10.00	±0.05	±0.41	±13.00	±0.06		±2.70	±3.70	

Γ_{gi} – FWHM of the Gaussian component, $i = 1, 2$; Γ_p – angle of cutoff of the θ–axis (angle) by the parabola; E_{gi} – energy of the annihilating pair, $i = 1, 2$; $S_{gi}/S_p/S_{sum}$ – area under Gaussian/parabola/total area, $i = 1, 2$; E_F – Fermi energy; $N_p(\theta)$ – density of the conduction band electrons.

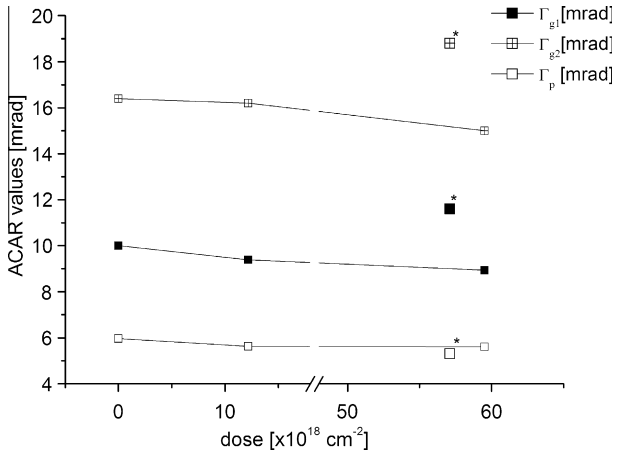

Fig. 4a. Width of the ACAR components (LP material).

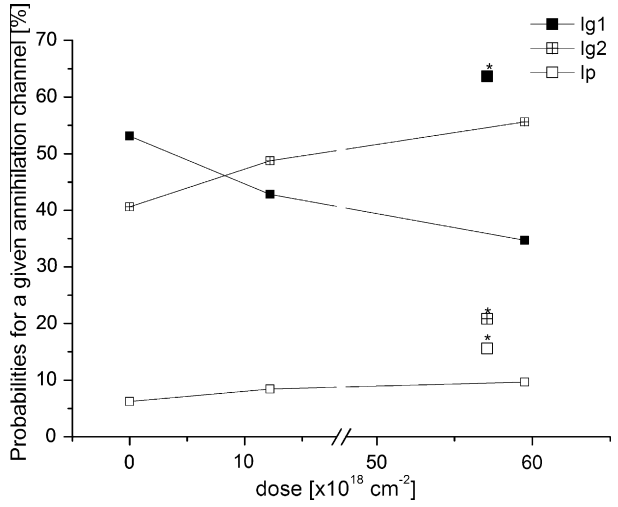

Fig. 4b. Intensities ($Ii = S_i/S_{sum}$) of the ACAR components (LP material).

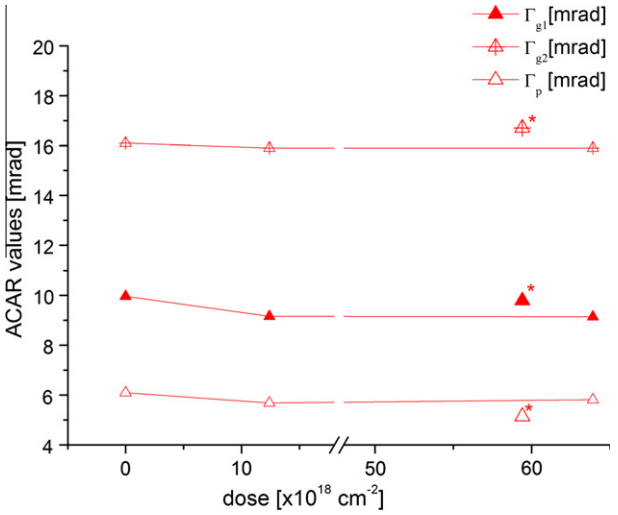

Fig. 5a. Width of the ACAR components (MP material).

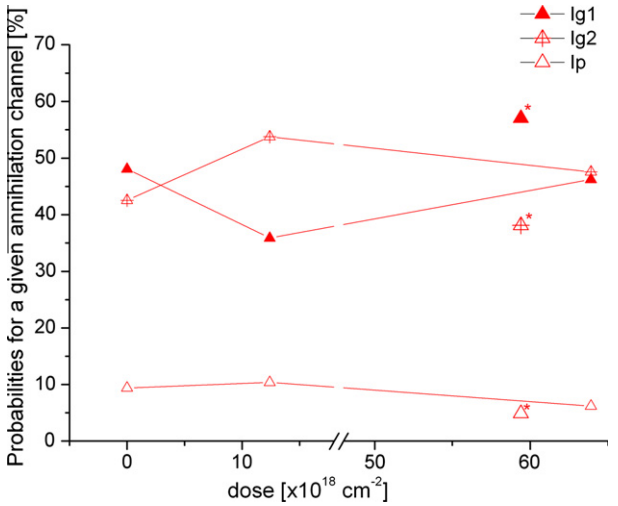

Fig. 5b. Intensities ($I_i = S_i/S_{sum}$) of the ACAR components (MP material).

To calculate the radiation-induced defect size, we used the ionization potentials of the neutral and single ionized metal atoms (Table 5 [18]). These elements represent more than 99 wt.% of VVER-440 weld material. As can be seen from experimental results, the energy of annihilating pairs (E_{g1} and E_{g2}) corresponds very well to the ionization potentials of Fe and Cr and with respect to

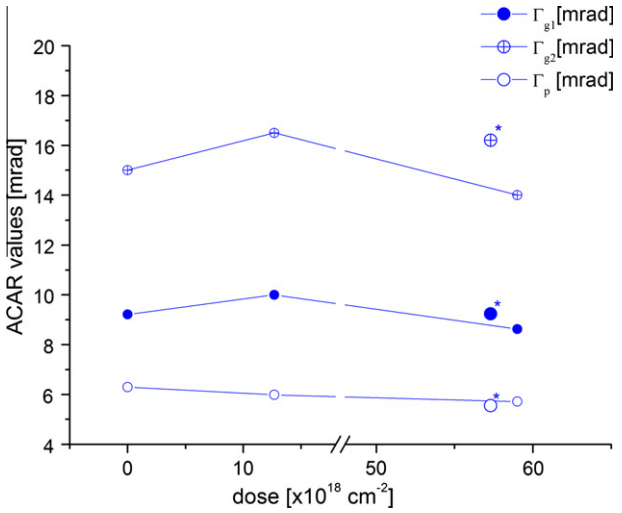

Fig. 6a. Width of the ACAR components (HP material).

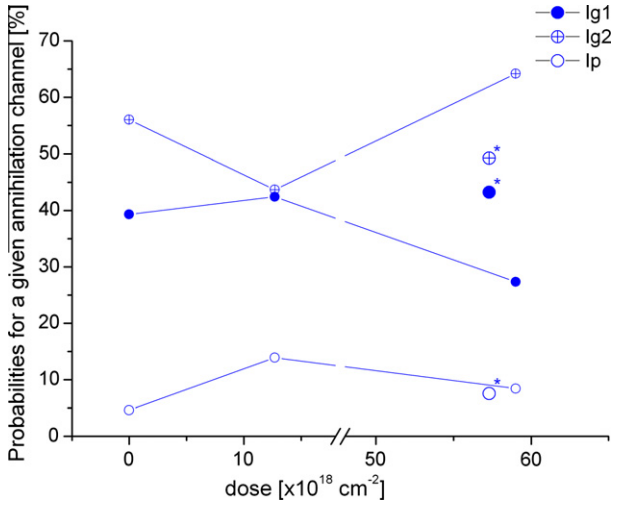

Fig. 6b. Intensities ($I_i = S_i/S_{sum}$) of the ACAR components (HP material).

chemical composition we can assume that annihilation takes place predominantly with the electrons of these atoms.

Based on the assumption that the general defect is correctly modelled as a potential well with infinitely high walls, the energy of the particle trapped in this defect can be expressed as $E = \frac{\pi^2\hbar^2}{2mR^2}$, where m is the mass of the particle, R is the radius of the potential well and $\hbar$ is the reduced Planck constant. So we can then express the size of the defect according to (1):

$$R_d = \sqrt{\frac{37.7}{E_{g1(2)} - E^{+(2+)}}}, \quad (1)$$

where R_d (Å) is the radius of the defect, $E_{g1(2)} = 6.9 \times 10^{-2} I^2_{g1(2)}$ (eV) is the energy of the annihilating electron–positron pair and $E^{+(2+)}$ is the first (second) ionization potential of Fe or Cr, respectively. $E_{g1(2)} - E^{+(2+)}$ is the energy of the annihilating positron. Since the radiation-induced defects are expected to be small agglomeration of vacancies, wider Gaussian component (E_{g2}) and second ionization potential of iron were used for the calculation of these defects.

Based on these calculations we can characterise the size of the radiation-induced defects in the irradiated materials to be 2–5.5 Å in radius, which can be assigned to clusters of 5–10 vacancies. The average value of ~4 Å observed in the studied materials after 3 years of irradiation, decrease to ~3 Å after subsequent annealing.

Let us assume that the positron trapping rate in these defects is determined only by their cross-section. Consequently, the positron trapping cross–section σ^+ (cm^2) in these defects can be defined as:

$$\sigma^+ = \pi R_d^2. \quad (2)$$

For mean values of defect size (4 Å) we can obtain the positron trapping cross-section as $\sigma^+ = 5 \times 10^{-15}$ cm^2.

Since it is impossible to distinguish all types of defects expected in the material, an additional assumption must be used that relates to the two main classes of defects. The first class of defects represents the dislocations which are present in the initial (non-irradiated) material, while the second class refers to radiation-induced defects [4].

An elementary examination of the kinetics of the annihilation process results in Eq. (3) for determining the mean value of the concentration of defects from the main characteristics of the annihilation spectra [13]:

$$\kappa_d N_d \cong \lambda_2 \cdot \Delta I_2 \cong \frac{\Delta I_2}{\tau_2}. \quad (3)$$

Here $\kappa_d = \sigma^+ v$ (cm^3 s^{-1}) is the positron trapping rate constant relating to radiation-induced defects, N_d is the concentration of these defects, ΔI_2 is the difference between the wide Gaussian components of the non-irradiated and irradiated sample ACAR spectra, $\lambda_2 = (\tau_2)^{-1}$ is the mean annihilation rate (lifetime) of the component describing the annihilation in non-irradiated sample as adopted from [11]. In the trapping rate constant, $v = \sqrt{8k_0T/(\pi m_+)} = 1.05 \times 10^7$ (cm s^{-1}) is the velocity of thermalized positrons (k_0 is the Boltzmann constant, T (K) is the temperature and m_+ is the positron mass).

Using these parameters, the concentration of radiation-induced defects in the irradiated materials can be defined by

$$\overline{N_d} = \frac{\Delta I_2}{\sigma_+ v \tau_2}. \quad (4)$$

Taking the mean size of radiation-induced defects (R = 4 Å) and the values calculated above, we find the concentration of the radiation-induced defects to be approximately 10^{16} cm^{-3}. These are average values for all the studied materials after 3 years of irradiation.

In the work of Kocik et al. [11], the mean size of the radiation-induced defects in VVER-440 weld material was characterized by a positron lifetime of ~260 ps (which corresponds to clusters of four vacancies ~R = 2.8Å). Taking the results from those experiments, we obtain the trapping rate $\kappa_d N_d \cong 0.06/1.5 \times 10^{-10}$ s^{-1} = 4×10^8 s^{-1}

Table 5
Ionization potentials of the elements of the materials studied [18].

Element	Fe	Cr	C	Si	Mn	P	S	Ni	Mo	Cu	V
E^+ (eV)	7.9[a]	6.76[a]	11.3	8.15	7.43	10.56	10.35	7.63	7.13	7.72	6.74
E^{2+} (eV)	16.2[b]	16.49[b]	24.4	16.34	15.64	19.65	23.4	18.15	15.72	20.29	14.65

[a] E_{g1} — non-irradiated samples (3 component spectra decomposition) ~ 5.86–6.91 (eV).
[b] E_{g2} — non-irradiated samples (3 component spectra decomposition) ~ 15.6–18.6 (eV).

and we find the defect concentration to be $2 \times 10^{16}\,\mathrm{cm}^{-3}$. Higher concentration of defects can be explained by the higher fluence ($10^{25}\,\mathrm{m}^{-2}$) of the irradiation treatment applied.

As mentioned above, the parabolic component of the spectra characterizes the annihilation with electrons from the conduction band. From this component, the values of Fermi energy (E_F) and density of conduction (free) electrons ($N_p(\theta)$) can be derived according (6) and (7) [13,16,17].

$$E_F = \frac{mc^2}{2}\Gamma_p^2 = 0.256 \cdot \Gamma_p^2, \tag{5}$$

$$N_p(\theta) = \frac{8\pi}{3}\left(\frac{mc^2}{h}\right)^3 \Gamma_p^3 = 5.942 \times 10^{20} \cdot \Gamma_p^3, \tag{6}$$

$$N_p(\theta) = 4.6 \times 10^{21} \cdot E_F^{3/2}. \tag{7}$$

where Γ_p is in mrad, E_F is in eV and N_p is in cm^{-3}. The calculated values are listed in Tables 2–4.

As can be seen from Tables 2–4 both the Fermi energy and the conduction electron density decrease with the neutron fluence and this decrease continues also after subsequent annealing. Both effects can be interpreted as an involvement of these electrons in new chemical bonds created in the material. We can assume that this phenomenon takes place preferably at the grain boundaries and these bonds can be assigned, besides others, to formation of carbide clusters and disk carbides as well as P and Cu rich clusters, observed by Rogozkin et al. using the atom probe technique [3]. Since segregation of P and precipitation of Cu forms relatively shallow positron traps in comparison to the other types of defects (vacancies, dislocations, grain boundaries etc.), more detailed characterization of these structures will be the objects of follow-up experimental works.

During annealing of the irradiated PRIMAVERA samples Fermi energy and conduction electron density did not return to the initial values of non-irradiated samples. These phenomena can be probably be explained by the low annealing temperature used, when only a part of covalent bonds (e.g. in the carbides) formed during irradiation, is broken. However, the chosen temperature is considered to be optimal for the VVER-440 materials in terms of annealing of the vacancy type of defects.

Performed ACAR investigation indicates also that in the case of high phosphorus steel (HP), the first year of radiation exposure at the typical VVER-440 operational conditions resulted in decreasing of the small vacancy type defects concentration. This effect can be, most probably, assigned to annealing of a part of originally higher concentration of these defects due to thermal and radiation exposure of steel samples. A similar effect, namely a decrease of the positron lifetime in VVER-440 base material after irradiation ($7.81 \times 10^{23}\,\mathrm{m}^{-2}$), has been observed with the PAS-LT measurements and published in [8]. We can argue that creation of new radiation-induced defects is here in competition with the annealing effect due to temperature and due to neutron irradiation.

4. Conclusions

Experimental investigation of the PRIMAVERA steel samples (VVER-440 weld materials) was carried out using positron annihilation spectroscopy – ACAR measurements. By evaluating the experimental results and correlating them with published data we were able to identify radiation-induced defects and to estimate their size and concentration.

Clear response of various phosphorus content materials to the radiation exposure has been recognized. A common feature of all irradiated materials is increased density of small radiation induced vacancy clusters ($R \sim 4$ Å) during the radiation exposure, recognized as a change of the intensity of the wide Gaussian component (I_2) in ACAR spectra. ΔI_2 between irradiated and non-irradiated sample sets varies from 5% to 15% during the total 3 years of irradiation.

PRIMAVERA project results indicate a possible role of phosphorus and copper in change of steel properties after irradiation. Positron trapping process is, however, not significantly affected by the presence of P and Cu clusters in the studied materials, since these are shallow traps for positrons comparing to other defects present in the material. Therefore the ACAR results allow to estimate the size and concentration of radiation-induced defects (nano-objects) and provide semi quantitative information on the new chemical bonds created in steel materials, while they do not allow to quantify specific role of P and Cu in these processes. The role of P and Cu should be therefore further studied in follow-up experimental works.

It is well known that post-irradiation annealing of the VVER-440 (base or weld) materials can result in significant decreasing of the radiation-induced defects and restoration of the mechanical properties. As demonstrated in the present paper, the performed thermal treatment (475 °C/100 h) decreases both the size and the concentration of vacancy agglomerates. This phenomenon is clearly visible in the case of LP material, where the material characteristics after annealing exceed the initial values. Annealing treatment of higher phosphorus content steel does not lead to full restoration of original properties.

Our study confirmed that PAS-ACAR technique can be with advantage applied in the investigation of the chemical bonds in the metallic materials. In the forthcoming experiments, the positron lifetime technique (PAS-LT) will be used to complete the investigation of the PRIMAVERA samples. This study allows a complex and comprehensive evaluation of irradiation effects on the VVER RPV materials, obtained by different experimental techniques, which can contribute to the development of the relevant embrittlement model.

References

[1] V. Slugen, D. Segers, P.M.A. De Bakker, E. De Grave, V. Magula, T. Van Hoecke, B. Van Waeyenberge, J. Nucl. Mater. 274 (1999) 273–286.
[2] A. Chernobaeva, J. Shtrombah, A. Krjukov, D. Erak, P. Platonov, J. Nikolaev, E. Krasikov, L. Debarberis, Yu. Kohopaa, M. Valo, Vodenicharov, Int. J. Pres. Vess. Pip. 84 (2007) 151–158.
[3] S. Rogozkin, A. Chernobaeva, A. Aleev, A. Nikitin, A. Zaluzhnyi, D. Erak, Ya. Shtrombakh, O. Zabusov, L. Debarberis, A. Zeman, in: Proceedings of Pressure Vessels and Piping Conference, Prague, July 2009, pp. 26–30.
[4] W.J. Phythian, C.A. English, J. Nucl. Mater. 205 (1993) 162.
[5] A. Zeman, L. Debarberis, L. Kupca, B. Acosta, M. Kytka, J. Degmova, J. Nucl. Mater 360 (2007) 272–281.
[6] V. Krsjak, V. Slugen, M. Miklos, M. Petriska, P. Ballo, Appl. Surf. Sci. 255 (2008) 153–156.
[7] M. Lambrecht, A. Almazouzi, J. Nucl. Mater. 385 (2009) 334–338.
[8] V. Slugen, G. Kogel, P. Sperr, W. Triftshauser, J. Nucl. Mater. 302 (2002) 89–95.
[9] V. Slugen, A. Zeman, J. Lipka, L. Debarberis, NDT E Int. 37 (2004) 651–661.
[10] V.N. Belyaev, V.V. Metelitsin, NIM-A 448 (2000) 89–93.
[11] J. Kocik, E. Keilova, J. Cizek, I. Prochazka, J. Nucl. Mater. 303 (2002) 52–64.
[12] V. Krsjak, W. Egger, M. Petriska, S. Sojak, Problem Atom. Sci. Technol. 4 (2009) 109–115.
[13] V. I Grafutin, E.P. Prokopev, Phys. – Uspekhi 45 (1) (2002) 59–74. 63.
[14] H.P. Leighly, Analytical Characterization Of Aluminum, Steel, And Superalloys, ISBN 0-8247-5843-9, 2005, pp. 667–668.
[15] P. Kirkegaard, N. J. Pedersen, M. Eldrup, PATFIT-88. Report RISO-M-2740, 1989.
[16] V.I. Grafutin, V.L. Grishkin, G.G. Myasishcheva, Yu.V. Funtikov, Phys. Solid State 40 (1998) 549.
[17] V.I. Grafutin, E.P. Prokopev, G.G. Myasishcheva, Yu.V. Funtikov, Phys. Solid State 41 (1999) 843.
[18] J. Klikorka, B. Hajek and J. Votinsky, Obecna a anorganicka chemie, Prague, second ed., 1989.